Conformation of Poly(styrenesulfonate) Polyions in the Presence of Multivalent Ions: Small-Angle Neutron Scattering Experiments

E. Dubois*,† and F. Boué

Laboratoire Léon Brillouin, CEA-CNRS, UMR 12, CE Saclay, 91191 Gif-sur-Yvette, France

Received May 31, 2000; Revised Manuscript Received February 22, 2001

ABSTRACT: Small-angle neutron scattering (SANS) experiments are used to study fully charged poly(styrenesulfonate) (PSS) polyions in the semidilute regime, in the presence of multivalent cations. PSSNa solutions with added Na^+, Ca^{2+}, or La^{3+} ions and PSSCa solutions with added Ca^{2+} ions are studied. The chain conformation of the single chain is directly measured by the zero-averaged contrast method. Fitting the scattered intensity with the wormlike chain model leads to the determination of the weight per unit length $1/a$ and of the persistence length l_p. The results can be separated in two regimes. *For low ionic strength in PSSNa solutions*, the chain remains wormlike, and l_p roughly varies as $I^{-1/3}$, I being the ionic strength calculated without counterion condensation. The conformation seems to be ruled mostly by I for both multivalent and monovalent cations. *For higher ionic strength in PSSNa solutions and for PSSCa solutions*, the chain is no longer wormlike if multivalent ions are added, the chain appears "thicker", and I is not the only parameter that controls the conformation. The phenomena are qualitatively identical for both Ca^{2+} and La^{3+} although a phase separation occurs for La^{3+} contrary to Ca^{2+}. The conformation changes may result from bridging phenomena between monomers or from counterions condensation, which leads to a more compact chain.

1. Introduction

Polyelectrolytes are polymers that dissociate into a charged polyion and counterions of opposite charge. The electrostatic charges induce long-range electrostatic interactions, which deeply modify and complicate the behavior of polyelectrolyte solutions when compared to the behavior of neutral polymers. Many theoretical and experimental works have been published about polyelectrolyte solutions. However, the theoretical works often deal with the dilute regime, easier to treat, while the experimental works deal with the semidilute one, often easier for experiments. Moreover, the behavior of polyelectrolytes is controlled by many parameters, among them the intrinsic stiffness of the chain, noted l_0, the linear charge density, the ionic strength, and the nature of counterions. In this framework, it is interesting to know the conformation of a single chain. We give here direct measurements of the Fourier transform of the latter, as measured by small-angle neutron scattering with appropriate labeling, which is a unique tool for that in the semidilute regime.

We consider here poly(styrenesulfonate) (PSS). This is a totally charged (i.e., there is one charge per monomer) and flexible chain. Its conformation has likewise already been studied in several experimental works.[1−6] These studies deal with PSSNa except for ref 4, which deals with a counterion different from Na^+, tetramethylammonium (TMA^+). The polymer is studied in the semidilute regime by different kinds of small-angle neutron scattering (SANS) measurements. As the chain conformation is assumed to be wormlike, two parameters are determined from the data: a, which is the inverse of the mass per unit length, and l_p, which is the total persistence length. These experimental works raise several difficulties: (i) the values of a are dispersed (from 1.7 to 2.5 Å); (ii) the condensation of the counterions is not always taken into account and not in the same way, in particular the fraction of free ions contributing to the ionic strength I is different; (iii) it seems that l_p varies like $I^{-0.33}$ whereas l_e (the electrostatic persistence length l_e assuming $l_e = l_p - l_0$) varies like $I^{-0.5}$.

Moreover, these results do not appear to be in full agreement with any theory. The model of Odijk−Skolnick−Fixman which predicts $l_e \sim I^{-1}$ is not appropriate for such flexible chains. Agreement with the theory of le Bret, where $l_p \sim C_p^{-1}$ at low C_p and $l_p \sim C_p^{-1/2}$ at large C_p, is claimed in refs 1 and 2 but not in ref 4. The simulations of Stevens and Kremer[7] also give underestimated persistence lengths compared with most experimental results including ours. In fact, no theory predicts that $l_p \sim I^{-0.33}$, as observed in refs 3 and 4. This relation could mean that l_p varies like the distance between monovalent ions, as suggested in ref 3.

To proceed in this controversial background, we chose to introduce in the solutions multivalent ions: a first way is to add to PSSNa solutions salts MCl_z of multivalent anions M^{z+}, which will mix with the Na^+ counterions. A second way is to neutralize PSSH solutions with calcium hydroxide, $Ca(OH)_2$, giving $(PSS)_2Ca$, id est divalent counterions; this is not possible for trivalent counterions since the $(PSS)_3M$ salt is not soluble (see below). These two procedures have several interesting features. First, with multivalent ions, the Debye length $\kappa^{-1} \sim I^{-0.5} = (0.5\sum_i c_i z_i^2)^{-0.5}$ and the distance between ions $d_i \sim \sum_i c_i^{-0.33}$ vary differently with c_i. This may help to understand which parameter controls l_p. Second, condensation should increase with the valence of counterions, and in the case of PSSNa with added $CaCl_2$ for example, added multivalent ions are supposed to replace the condensed monovalent ions. This may allow us to answer the question whether condensation of counte-

* Corresponding author. Tel 33 1 44 27 32 67; Fax 33 1 44 27 38 34; E-mail emdubois@ccr.jussieu.fr.

† Present address: Laboratoire Liquides Ioniques et Interfaces Chargées, UMR 7612, 4 place Jussieu, case 51, 75252 Paris Cedex 05, France.

10.1021/ma000956u CCC: $20.00
Published on Web 04/26/2001

rions has to be taken into account when calculating the ionic strength or not. However, the presence of multivalent ions may induce effective attractions between charged sites of the chain segments, phenomena that we expect to be negligible for small concentrations of added multivalent ions, especially with divalent counterions. If such effects are no more negligible, i.e., if multivalent ions interact strongly enough with the polyions (for the large added salt concentrations and high valence), this may lead to gelation or phase separation of the solutions. Such phenomena are very important to know and to control because multivalent ions are widely used for industrial applications. Several authors have studied the macroscopic phase diagram of polyelectrolytes with multivalent ions.[8−11] Nevertheless, such macroscopic studies only give access to a value of destabilization threshold if it exists, but not directly to the evolution of the chain conformation.

The study of the chain conformation in these different situations can be performed using SANS. To study all monophasic solutions, we thus take advantage here of the zero-averaged contrast method (ZAC, see section 2.4), which allows us to directly measure the chain form factor even in the semidilute regime. In the present article, most of the data deal with PSSNa with added salt. We first consider the addition of divalent calcium ions to PSSNa solutions (section 3): the addition of Ca^{2+} ions does not induce destabilization. Then we consider the addition of trivalent lanthanum ions La^{3+} (section 4), which, on the contrary, leads to a phase separation above a first threshold of salt concentration followed by a redissolution above a second threshold.[9,11] Effects of the additions of Ca^{2+} and La^{3+} are then compared (section 5) and compared with addition of monovalent Na^+ ions (section 6). Finally, some preliminary results are reported on PSSCa with or without added Ca^{2+} (section 7). We show that they enlighten the PSSNa results (section 8).

2. Experimental Methods

2.1. Polymer. Monodisperse normal (i.e., nonperdeuterated) polystyrene (h-PS, $M_w = 67\,500$, $M_w/M_n = 1.03$) and perdeuterated polystyrene (d-PS, $M_w = 73\,000$, $M_w/M_n = 1.04$) are purchased from Polymer Standard Service (Mainz, Germany). The Vink's method[12] is used to prepare totally sulfonated polystyrene (PSS). The poly(styrenesulfonic acid) obtained is neutralized by NaOH to obtain PSSNa or by $Ca(OH)_2$ to obtain PSSCa. (Note that, for simplicity, we always write PSSCa in the following, although one Ca^{2+} ion neutralizes two sulfonate groups, so that it could be written $PSSCa_{1/2}$.) All samples are then carefully dialyzed against deionized water until the conductivity of the bath remains stable. The solutions are then concentrated with a rotational evaporator and finally freeze-dried, which leads to a white powder stored at 4 °C.

The solutions, prepared by dissolving the polymer in the desired solvent (mixture of H_2O and D_2O suitable to the ZAC method), are stirred for 24 h and filtered on a 0.22 μm filter (Millipore). The polymer concentration is then checked by titration of the carbon in the sample (COT, total organic carbon, Dohrmann). All the experiments are performed in the semidilute regime, and the equivalent monomer concentrations c_P studied lie between 0.076 and 0.3 mol/L.

2.2. Ionic Strength and Condensation. The solutions are constituted of polymer PSSM with a counterion M of charge z_{ci} and an added salt noted XCl_z, z being the charge of the cation X. Both the counterions of the polymer chain and the free ions in solution contribute to the ionic strength I. Nevertheless, parts of the counterions are usually considered to be condensed on the chain.[13,14] For a polymer totally sulfonated, the distance between ionized groups before condensation is the size a of the segment. There is condensation of counterions if $a/z_{ci}l_B < 1$, where l_B is the Bjerrum length, and this leads to an effective charge $f_{eff} = (1/z_{ci})(a/l_B)$. Moreover, if multivalent ions are added to a polymer with monovalent counterions, the multivalent ions are supposed to replace the monovalent ones initially condensed.

If I is calculated without taking condensation into account, $I = 0.5\{x_{ci}^2(c_P/z_{ci}) + z^2c_s = zc_s\}$, where c_p is the polymer concentration and c_s the added salt concentration. This leads here to $I = c_p/2 + z(z + 1)c_s/2$ for PSSNa with XCl_z and to $I = c_p + 3c_s$ for PSSCa with $CaCl_2$.

On the contrary, assuming theoretical values (Manning) of the number of counterions condensed, $I_{cond} = ac_p/2l_B + c_s$ for PSSNa with NaCl and $I_{cond} = ac_p/2l_B + 3c_s$ for PSSCa with $CaCl_2$. For PSSNa and multivalent added salts, in the framework of the simplest model, three regions can be distinguished. If the condition $c_s < c_p(1 - a/l_b)/z$ is met, then the condensed Na^+ ions are replaced by condensed multivalent ions and $I_{cond} = ac_p/2l_b + zc_s$; when this is completed, condensation of multivalent ions continues until $c_s = c_p(1 - a/zl_b)/z$, and the ionic strength is given by $I_{cond} = (c_p + zc_s)/2$. If the condition $c_s > c_p(1 - a/zl_b)/z$ is met, then the multivalent ions added stay in the solution, and the ionic strength is given by $I_{cond} = (1 - z)/2c_p + z(z + 1)c_s/2 + ac_p/2l_b$.

However, the above evaluation of the contribution of condensed counterions to the ionic strength can be questionned, which is a first difficulty in calculating the ionic strength. A second difficulty arises from the choice of the value of the distance a as we shall see below.

2.3. Small-Angle Scattering Experiments (SANS). SANS measurements are performed on two instruments: PACE (Orphée reactor, CEA-Saclay, France) for the higher concentrations and D22 (ILL, Grenoble, France) for all other samples. Two settings are used in each case. On PACE, the two settings $D = 0.92$ m, $\lambda = 5$ Å and $D = 3.02$ m, $\lambda = 12.5$ Å cover a range of values of scattering vector modulus ($q = 4\pi/\lambda \sin(\theta/2)$) between 5×10^{-3} and 0.4 Å^{-1}. On D22, $D = 5$ m, $\lambda = 10$ Å and $D = 1.5$ m, $\lambda = 10$ Å cover a q range between 5×10^{-3} and 0.3 Å^{-1}. The quartz cells are 2 mm thick for all samples except for light water (1 mm). The temperature has been kept constant at 25 °C during all experiments.

2.4. Zero Average Contrast Method (ZAC): Form Factor.[1,3,15,16] Let us consider a mixture of d-PSS and h-PSS, of total volume fraction Φ_T, with $\Phi_D\Phi_T$ of d-PSS and $(1 - \Phi_D)\Phi_T$ of h-PSS in a given solvent. If k_H and k_D (cm) are the contrast between respectively h-PSS and d-PSS and the solvent, the scattered intensity is

$$I(q)\ (\mathrm{cm}^{-1}) = (1/V)\ \mathrm{d}\sigma/\mathrm{d}\Omega = [(1 - \phi_D)k_H^2 + \phi_D k_D^2]S_1^*(q) + [(1 - \phi_D)k_H + \phi_D k_D]^2 S_2^*(q) \quad (1)$$

where $S_1^*(q)$ (cm^{-3}) is the intrachain signal and $S_2^*(q)$ is the interchain signal. $S_1^*(q)$ corresponds to the chain form factor, i.e., to the correlations between monomers of the same chain. $S_2^*(q)$ corresponds to the correlations between monomers of two different chains.

If $\Phi = 0.5$ and $k_H = -k_D$, eq 1 reduces to $I(q) = k_H^2 S_1^*(q)$, thus allowing a direct measurement of the form factor of 1 chain among the others, even in the semidilute regime, without need for any extrapolation. In the case of PSS, $k_H = -k_D$ in a solvent constituted of 29% H_2O and 71% D_2O.[6,16] This method is nevertheless only valid if the contributions of the counterions to the intensity is negligible. This point has been detailed in the Appendix.

If h-PSS alone is dissolved in water, eq 1 reduces to $I(q) = k_H^2 S_T^*(q)$, where $S_T^*(q) = S_1^*(q) + S_2^*(q)$ is the so-called total signal. For hard spheres, undeformable, centrosymmetric, $S_T^*(q)$ can be written $NP(q)S(q)$, where $NP(q) = S_1(q)$, $P(q)$ being the form factor and $S(q)$ the structure factor linked to the distribution of the centers of the spheres, and which tends toward 1 at large q. By analogy with hard spheres, we will

consider the ratio S_T/S_1 which corresponds to an "apparent structure factor" and should also tend toward 1 at large q.

For a better readability, we shall later use the intrachain signal $S_1(q)$ (mol^{-1}) $= S_1^*(q)/c_p = I(q)/c_p k_H^2$ (i.e., the form factor), and the total signal $S_T(q) = S_T^*(q)/c_p$.

For small scattering vectors, i.e., $qR_g < 1$, the form factor $S_1(q)$ verifies the following expression:

$$\frac{1}{S_1(q)} = \frac{c_p k_H^{\ 2}}{I(q)} = \frac{1}{0.0006N}\left(1 + \frac{q^2R_g^2}{3}\right) \tag{2}$$

where c_p is the monomer concentration (mol/L), N the number of monomer per chain, and R_g the radius of gyration (Å). This allows us to determine both the weight of the polymer (through N) and R_g.

2.5. Data Treatment. The data are normalized using the incoherent scattering of light water, the latter being calibrated to obtain absolute values of $(1/V)(d\sigma/d\Omega)_{water}$ in cm^{-1}, and the solvent contribution is subtracted from these values.

At small q, the greatest difficulty is the existence of aggregates. They indeed contribute to the intensity in the low q range, which increases $I(q)$, and R_g and N may be overestimated when using the Zimm method following eq 2. If the polymer solutions are not filtered, the aggregates lead to an intensity decreasing as q^{-x} with $3 < x < 4$ for small q. This contribution is different for all samples and prevents us from using eq 2 and also from fitting the data according to the procedure explained in section 2.6. If the polymer solutions are filtered (see section 2.1), the intensity at low q tends toward the weight of the polymer (N). Nevertheless, it is difficult to be sure that there is no contribution of the aggregates. The measurement of the weight of the polymer gives a good order of magnitude (see section 3.2) with a large dispersion (around 20%). This can result both from the error on our measurements and from the presence of aggregates. For the same reasons, the error on R_g is around 30%. A remedy to this difficulty is to use the whole fit of the curve (see section 2.6) to determine R_g.

At large q the difficulty is to evaluate the incoherent background. At this stage several factors are difficult to evaluate. First, water always remains adsorbed on the PSS polymer (around 10% in weight, i.e., around one water molecule per monomer). This introduces some error on the polymer concentration. Second, the filtration of the solutions may also change their concentration. These two points are the reasons why the concentration is determined in the filtered solution. The accuracy on these determination is around 5%. Third, it is quite difficult to estimate the incoherent background due to the polymer chain itself. Finally, although the solutions are prepared precisely and with great care, some deuterium atoms in the water may be exchanged by hydrogen atoms by contact with air, leading to an error on the background level. As the intensity is very small, especially for large q ($q > 0.2$ Å^{-1}, $I < 0.05$ cm^{-1}), compared to the background ($\sim$1 cm^{-1}), all these problems make us unable to know the exact quantity to subtract with an accuracy better than 3%. It has little influence for small q but can lead to very different shapes for large q. This is why we decide to take as a reasonable criterion that the intensity decreases as q^{-1} for large q, assuming that the chain behaves like a rigid rod (with no lateral size) for such small scales. This gives us a precise value for the intensity background.

2.6. Fit of the Whole Form Factor. The experimental curves are fitted with the wormlike chain model (WLC). Reference 15 is dedicated to this procedure. In this WLC model the chain is rodlike for small scales and follows a random walk for large scales. It is characterized by two parameters: the persistence length l_p and the number of elementary units per length $1/a$ (a is an apparent monomer length, in other words the contour length $L = Na$). They may be obtained from the fit of the data using the different theoretical expressions that have been derived depending on the q range.[6] For $ql_p < 2$, as derived by Sharp and Bloomfield,[17] we used

$$S_1(q) = 6 \times 10^{-4}N\left[\frac{2(e^{-x} + x - 1)}{x^2} + \frac{2l_p}{Na}\left[\frac{4}{15} + \frac{7}{15x} - \left(\frac{11}{15} + \frac{7}{15x}\right)e^{-x}\right]\right], \quad \text{with } x = Naq^2l_p/3 \tag{3}$$

For $ql_p > 4$, we use the asymptotic expression derived by des Cloizeaux:[18]

$$S_1(q) = 6 \times 10^{-4}\left[\frac{\pi}{qa} + \frac{2}{3q^2al_p}\right] \tag{4}$$

which is independent of N. In the q range between these two limits, we use a numerical function derived by des Cloizeaux,[18] which may be approximated by an analytic expression:

$$S_1(q) = \frac{6 \times 10^{-4}}{q^2}\frac{1}{al_p}(6 + 0.547(ql_p)^2 + ...) \tag{5}$$

The fit is usually performed using a representation $q^2S_1(q)$ vs q, because the changes are visualized more easily. Figure 1a shows an example of this representation for measured data and for the three theoretical expressions in their range of validity. For $q > 4/l_p$ (zone 3), in the asymptotic regime, $q^2S_1(q)$ is the line of slope $1/a$ that directly yields a (if S_1 is in absolute units). For $2/l_p < q < 4/l_p$ (zone 2), the extrapolation of the des Cloizeaux function for small q is proportional to $1/al_p$, thus leading to the product al_p if S_1 is in absolute units. For $q < 2/l_p$ (zone 1), $q^2S_1(q)$ depends on l_p, a, and the polymer mass, and the limit for $q = 0$ is proportional to N as explained above in section 2.4. The values obtained for l_p and a are related to the radius of gyration R_g using

$$R_{g,calc}^2 = \frac{Nal_p}{3}\left[1 - \frac{3l_p}{Na}\left(1 - \frac{2l_p}{Na}\right) - \frac{6l_p^3}{(Na)^3}\left(1 - \exp\left(-\frac{Na}{l_p}\right)\right)\right] \tag{6}$$

for a monodisperse mass distribution, where $Na = L$ corresponds to the total length of the chain.[1] The expression for a polydisperse distribution is given in ref 1.

Therefore, one has first to decide upon the value of a from the asymptote. Given that N is known from other measurements or from the extrapolations to $q = 0$ and that it is supposed to be the same for all the solutions, the value of l_p is then deduced from the low q and the middle q regions.

It is important to note that the data treatment performed as described in section 2.5 assumes that the wormlike chain model (WLC) is valid. Nevertheless, this procedure raises several difficulties. First, the scattered intensity is very small for large q, and it is difficult to subtract the background, as explained in section 2.5. A small difference in this subtraction induces very large differences on the parameter a, and consequently, the l_p value is also affected, as shown in Figure 1b: the same data as in Figure 1a have been treated by subtracting 2% more background. The large q region is no longer linear. Nevertheless, if one attempts to fit the data, this leads to $l_p = 46$ Å and $a = 2$ Å, parameters quite different from the values $l_p = 55$ Å and $a = 1.7$ Å found in Figure 1a. Second, the procedure described is no more possible to apply if l_p is too small because the asymptotic regime corresponds to very high q values, as shown in Figure 1c. In this case, the procedure of treating the data (section 2.5) in order to obtain a q^{-1} variation at high q is no more valid. Third, in some cases the WLC model can fit either the beginning or the end of the curve, as shown in Figure 1d. In such situations, we conclude that the chain is not wormlike.

3. Addition of Ca^{2+} Ions to PSSNa

A first experiment, which is easy, is to add Ca^{2+} ions through the addition of $CaCl_2$ in a PSSNa solution in order to compare to the previous experiments dealing

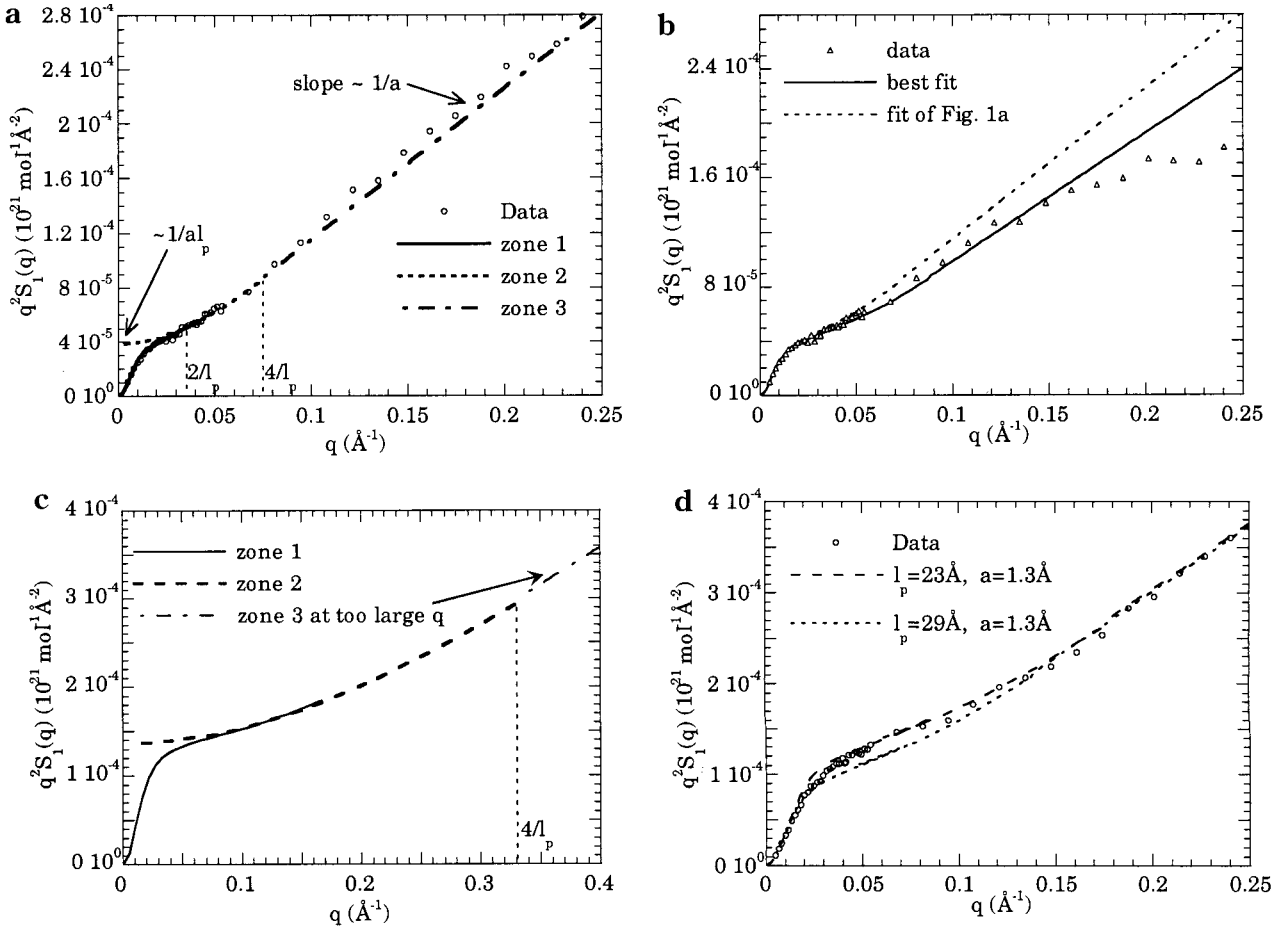

Figure 1. (a) Typical q^2S_1 vs q plot used for the fitting of the data. The experimental data correspond to PSSNa with $c_p = 0.3$ mol/L and no added salt. The three zones correspond to the three theoretical expressions used depending on the q range, as described in section 2.6. The fitting parameters are $l_p = 55$ Å and $a = 1.7$ Å. (b) Same data as in Figure 1a treated by subtracting 2% more background. The line is the best fit and corresponds to $a = 2$ Å and $l_p = 46$ Å. The dots correspond to the fit of Figure 1a ($a = 1.7$ Å and $l_p = 55$ Å). (c) Theoretical curve for $a = 1.7$ Å and $l_p = 12$ Å. (d) Example of data that cannot be fitted with the wormlike chain model: the two calculated curves show the region where the model fails.

Table 1. Addition of Divalent Calcium Ions in PSSNa Solutions: Parameters Determined by Fitting SANS Experiments to the Wormlike Chain Model[a]

[Ca] (mol/L)	c_p (mol/L)	N	R_g (Å)	I (mol/L)	a (Å)	l_p (Å)
0	0.305	860	180	0.15	1.7	55
0.037	0.28	739	158	0.25	1.6	52
0.11	0.305	840	148	0.48	1.6	36
0.25	0.28	808	139	0.89	not wormlike	
0.5	0.305	828	126	1.65	not wormlike	
1	0.28	811	124	3.15	not wormlike	
0.028	0.165	682	177	0.17	1.6	70
0.14	0.165	658	136	0.5	1.6	36
0.012	0.076	744	180	0.075	1.6	77
0.028	0.076	799	166	0.12	1.5	62
0.125	0.076	715	123	0.42	1.5	38

[a] c_p is the polymer concentration; the ionic strength I equals $c_p + 2c_s$.

with the addition of NaBr in PSSNa.[3] The solution remains macroscopically stable for all $CaCl_2$ concentrations, but the introduction of divalent ions should change the condensation phenomena on the polyion as well as the evolution of the ionic strength with salt concentration. The polymer concentrations used are $c_p \sim 0.3$, 0.16, and 0.075 mol/L. All the results are reported in Table 1; however, only selected data are plotted in Figures 2 and 3 in order to keep the graphs readable. Moreover, all the data for $S_1(q)$ and $S_T(q)$ are available on request at the Publisher Office.

3.1. Total Scattering S_T in Full Contrast. The intensity corresponding to "total scattering", i.e., to full contrast conditions, is plotted for several samples in Figure 2a for $c_p \sim 0.3$ mol/L. The curve with no added Ca shows a maximum. It results from the electrostatic repulsion between chains: the latter leads to a low compressibility and thus to a low intensity at small q, i.e., to a peak in between the low and the high q regime.[19] The abscissa q_{max} associated with the peak can be related to a mean distance between chains $d = 2\pi/q_{max}$, in analogy with charged spheres in water. In the semidilute regime without salt, $q_{max} \sim c^{0.5}$, a relation known for a long time,[20] checked by many authors and found in the present study for the solutions without added salt. If $CaCl_2$ salt is added, the repulsion is screened and the peak disappears before any clear change in q_{max}.

At very low q, when $q \rightarrow 0$, it is important to notice the strong upturn of intensity (in practice for $q < 0.03$ Å^{-1}). This corresponds to some aggregate contribution, which decreases after filtration of the solutions but was never suppressed in our data. When adding $CaCl_2$, the part of the intensity that corresponds to these aggregates remains roughly constant, as shown in Figure 2a.

In summary, the phenomena observed with addition of calcium salt are qualitatively the same as the ones observed on the same PSSNa with addition of sodium

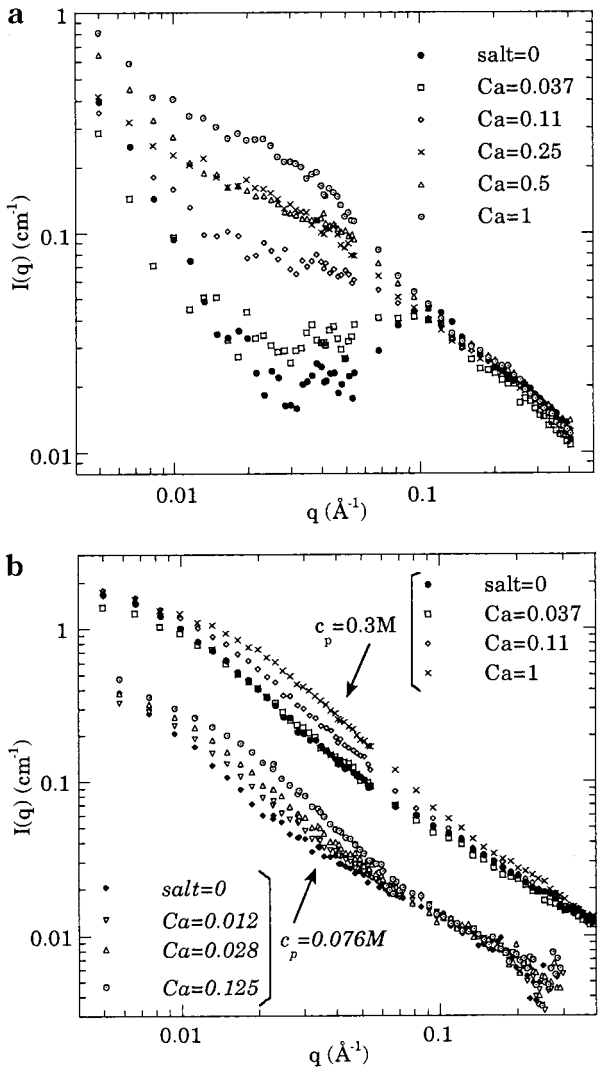

Figure 2. Addition of Ca^{2+} in PSSNa solutions: scattered intensity as a function of q. The Ca^{2+} concentrations are given in the legend (mol/L). (a) Full signal S_T with $c_p = 0.3$ M. (b) Form factor S_1 with $c_p = 0.3$ M and $c_p = 0.076$ M.

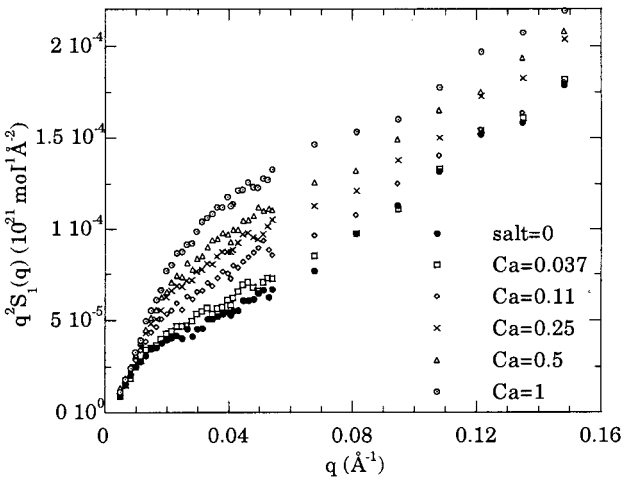

Figure 3. Addition of Ca^{2+} in PSSNa solutions; Kratky representation of the form factor: q^2S_1 as a function of q. $c_p = 0.3$ M, and the calcium concentrations are given in the legend (mol/L).

bromide[3,13] or other polymers with addition of sodium chloride.[21] We can infer that the structure of the solution

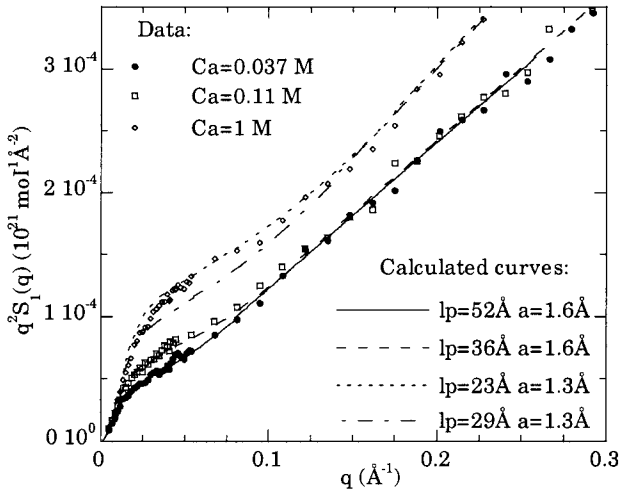

Figure 4. Addition of Ca^{2+} in PSSNa solutions. The dots correspond to experimental points for $c_p = 0.3$ M and different calcium concentrations (see legend). The lines correspond to the fit of the different curves (see l_p and a in the legend).

is similar. In other words, there is no severe perturbation of the solution when adding $CaCl_2$.

3.2. Form Factor S_1. Figure 2b plots the intensity measured in ZAC conditions for two polymer concentrations. The curves extrapolate to the same value at small q as expected since it corresponds to the polymer molecular weight; they are also nearly superimposed at large q where all the curves should vary as $1/qa$ according to the wormlike chain model. The changes in the middle of this q range are easier to visualize in the Kratky representation as shown in Figure 3.

Table 1 reports the results for N and R_g determined from S_1 for all the performed experiments with added $CaCl_2$. The values of N are quite dispersed around a mean value of 770. For the initial PS chains (before sulfonation), $N = 650$, and it is known that N slightly increases after the sulfonation step. Here, $N = 760$ according to a SEC (size exclusion chromatography, performed in the SCM, CEA-Saclay) determination for PSSNa. The large dispersion of the values obtained from SANS (Table 1) is probably due to the increase of intensity in the small q range, due to the aggregates that remain despite the filtration and that are different in each sample (see section 2.5).

The parameters a and l_p, which characterize the chain conformation, are obtained from the fit of the whole curve (Table 1). Three cases are plotted in Figure 4. At low Ca^{2+} concentration (0.037 and 0.11 mol/L), the curves are well fitted with the wormlike chain model. On the contrary, at high Ca^{2+} concentration, the curve cannot be satisfactorily fitted in the frame of this WLC model. The chain thus seems to be no longer wormlike. It is also noticeable that the parameter a needed for the fitting attempts is much smaller than for low Ca^{2+} concentrations ($a = 1.3-1.4$ Å instead of $a = 1.6-1.7$ Å), suggesting a conformation change. Once a is chosen, we can either fit the beginning of the curve, i.e., R_g, or the middle, i.e., l_p, but not both together, as shown in Figure 4.

In summary, two regimes can be distinguished for the addition of calcium ions in PSSNa. For ionic strengths lower than 0.5 mol/L ($I = c_p/2 + 3c_s$ calculated without taking condensation into account, see section 2.2), the WLC model seems to be relevant. For ionic strengths larger than 0.5 mol/L, the curves cannot be fitted in the

framework of the WLC model and this point will be discussed later (sections 6.5 and 8).

4. Addition of La^{3+} Ions to PSSNa

We have performed in PSSNa the same measurements with trivalent La^{3+} ions (through addition of $LaCl_3$) as with Ca^{2+} ions, when the solutions are stable. This is not always the case since the addition of trivalent ions (or ions of higher valence) leads to a phase separation above a threshold $[La^{3+}]_1$, before dissolving again above a second threshold $[La^{3+}]_2$.

Several authors[9,11] have built the phase diagram: the solutions are stable until a threshold $[La^{3+}]_1$, which roughly corresponds to the displacement of all Na^+ counterions condensed by La^{3+} ions, and there is a redissolution which leads to a monophasic solution because the electrostatic interactions are totally screened above $[La^{3+}]_2$. For the PSSNa studied here at room temperature ($T = 25$ °C), we have measured $[La^{3+}]_1 = 0.24c_p \pm 0.015$ (mol/L) and $[La^{3+}]_2 = 0.42 \pm 0.015$ mol/L. Then we have explored the polymer conformation in the stable regions: under $[La^{3+}]_1$ (typically $[La^{3+}] = 0.3$, 0.6, and $0.9[La^{3+}]_1$) to follow the changes until destabilization and above the redissolution threshold $[La^{3+}]_2$.

The full signal and the form factor measured are plotted in Figure 5. The trends are the same for the two polymer concentrations and qualitatively similar at first sight to what is observed for the addition of calcium ions. The results for N and R_g, reported in Table 2, are also perturbed by the aggregates. The parameters a and l_p are determined by fitting the curves of Figure 6, and the results are given in Table 2. Like in the case of calcium ions, the wormlike model is pertinent only for low La^{3+} concentrations. Above the $[La^{3+}]_2$ threshold, Figure 6b shows that the conformation seems mainly independent of the La^{3+} concentration as well as of the polymer concentration. The chain is quite contracted, as can be seen from the R_g value; at the same time, it is no longer wormlike.

5. Comparison between La^{3+} and Ca^{2+} Addition Effect

Although the lanthanum ions induce a macroscopic phase separation contrary to calcium ions, the microscopic behavior derived from the SANS experiments (in the monophasic region of course) are analogous for calcium and lanthanum. Indeed, adding salt screens the electrostatic repulsion, leading to a more compact and flexible chain: R_g and l_p decrease. Further, the WLC model used for low salt concentrations fails in both cases for high salt concentrations. The addition of multivalent ions seems to induce a change in the type of conformation at high enough salt concentrations, not only for lanthanum but also for calcium.

If the types of observed behaviors are qualitatively similar, it is however interesting to notice that, quantitatively, they correspond to extremely different salt concentrations. This can be seen by comparing Figures 2 and 5 and Figures 3 and 6: the conformation for $[La^{3+}] = 0.053$ mol/L and $[Ca^{2+}] = 1$ mol/L is nearly the same although the ionic strength is much higher for calcium. The ionic strength I (without condensation) is indeed 6 times higher for calcium than for lanthanum and I_{cond} (with condensation) is 15 times higher. This allows us to choose between two origins of the difference in the phase behavior with calcium and lanthanum. One could be that there is no effect at all in calcium and an effect only in lanthanum. A second one is that the effect exists already for the divalent case but is not strong enough to induce phase separation. Our result at the nanometric scale favors the second situation.

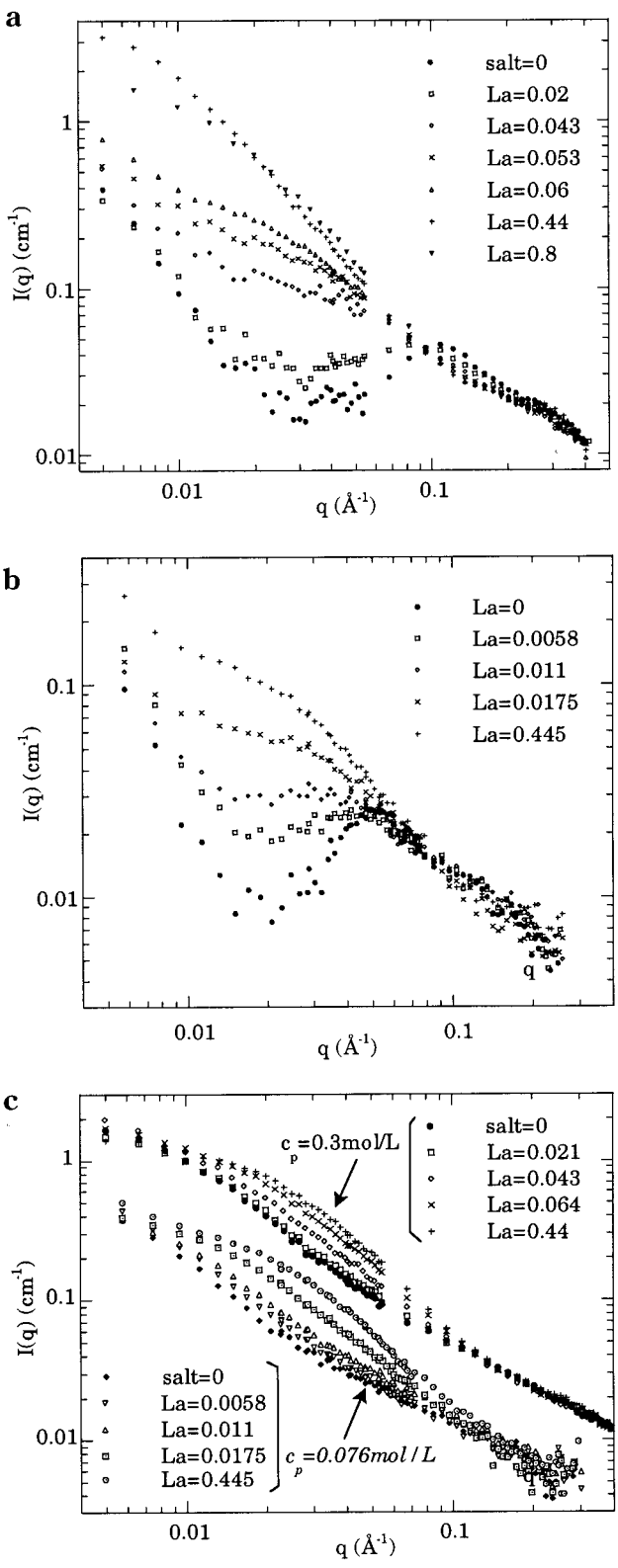

Figure 5. Addition of La^{3+} in PSSNa solutions: scattered intensity as a function of q. The La^{3+} concentrations are given in the legend (mol/L). (a) Full signal S_T with $c_p = 0.3$ M. (b) Full signal S_T with $c_p = 0.076$ M. (c) Form factor S_1 with $c_p = 0.3$ M and $c_p = 0.076$ M.

Table 2. Addition of Trivalent Lanthanum Ions in PSSNa Solutions: Parameters Determined by Fitting SANS Experiments to the Wormlike Chain Model[a]

[La] (mol/L)	c_p (mol/L)	N	R_g (Å)	I (mol/L)	a (Å)	l_p (Å)
0	0.305	860	180	0.15	1.7	55
0.021	0.28	800	154	0.26	1.6	49
0.043	0.26	924	144	0.38	not wormlike	
0.053	0.26	817	119	0.45	not wormlike	
0.064	0.28	834	121	0.52	not wormlike	
0.44	0.28	754	91	2.8	not wormlike	
0.8	0.25	742	98	4.9	not wormlike	
0.0058	0.076	1038	229	0.075	1.6	88
0.011	0.76	760	166	0.105	1.4	70
0.0175	0.076	711	119	0.29	not wormlike	
0.445	0.076	682	91	2.7	not wormlike	

[a] c_p is the polymer concentration; the ionic strength I equals $c_p + 2c_s$.

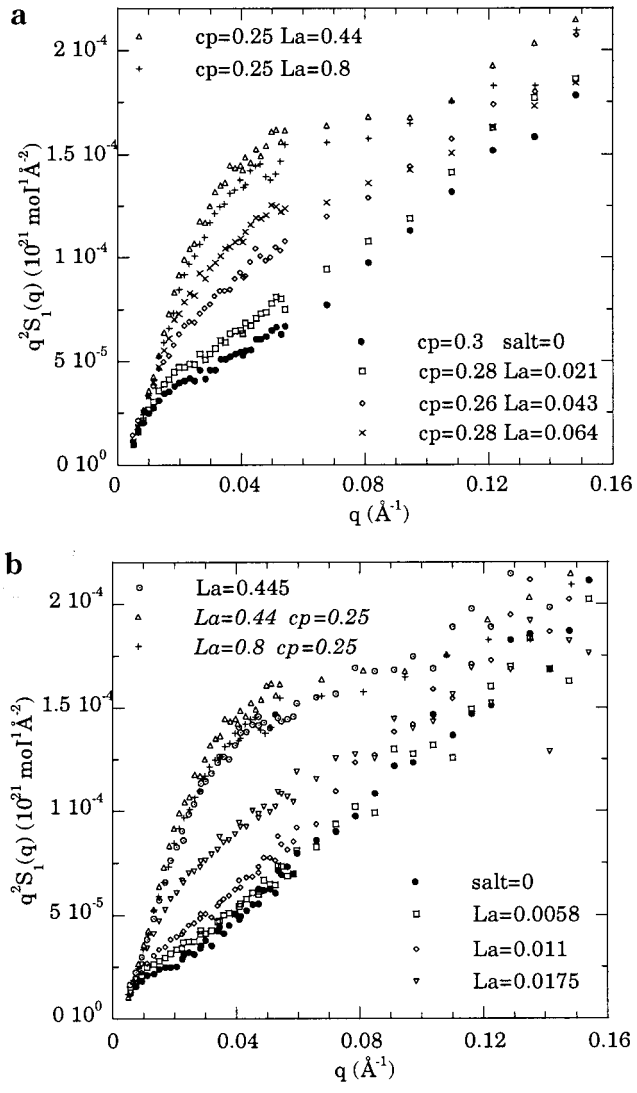

Figure 6. Addition of La^{3+} in PSSNa solutions; Kratky representation of the form factor. (a) c_p and $[La^{3+}]$ are given in the legend (mol/L). (b) $[La^{3+}]$ is given in the legend (mol/L) and $c_p = 0.076$ M except for two curves (see legend), plotted for comparison.

For all electrolyte concentrations for which the scattered intensity in ZAC conditions cannot be fitted by the WLC model, the hypothesis used for the subtraction of background (i.e., assuming $I \sim q^{-1}$ at large q) may be contested. As explained in section 2.6., such a situation may occur if the asymptotic regime ($q > 4/l_p$)

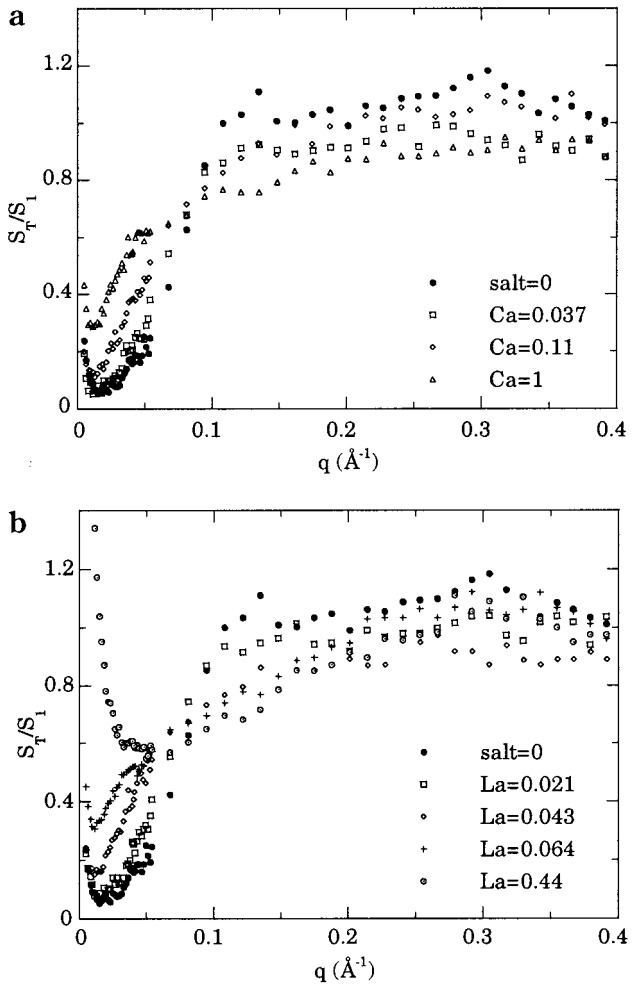

Figure 7. Ratio S_T/S_1 as a function of q for PSSNa solutions with $c_p = 0.3$ M: (a) addition of calcium; (b) addition of lanthanum. The salt concentrations are given in the legend (mol/L).

is not reached in our available q range (Figure 1c), i.e., for very low l_p, around 12 Å ($4/l_p \sim 0.33$ Å^{-1}), a value which corresponds to the one of polystyrene.[1] The data thus have to be treated differently, so that the intensity varies as q^{-x} with $x > 1$. We therefore undertook to subtract more background using a trial-and-error procedure for all samples. We concluded that this would be meaningful only for solutions with a lanthanum concentration above the redissolution threshold $[La^{3+}]_2$. In this case, subtracting more background can indeed improve the fit; this leads to x values larger than one and to $a = 1.7$ Å, $l_p = 12$ Å if keeping the same a value than the polymer without salt or to $a = 2.2$ Å, $l_p = 14$ Å, for the value of a used in ref 2. This seems realistic because the electrostatic interactions are totally screened for such high salt concentrations, and the polymer conformation should be close to the neutral chain.

The additions of divalent and trivalent ions may also be compared through the ratio S_T/S_1, which is plotted in Figure 7 for calcium and lanthanum. It tends toward 1 for large q values, which means that the q^{-1} variations of the total signal and of the form factor are superimposed. There is no influence of the interactions in this scale range, which corresponds to the scale of monomer, where the chain is rodlike. At small q, S_T/S_1 increases with q; the curve globally increases while adding salt, showing that the electrostatic repulsion is screened by the added ions. Nevertheless, all these curves present

an upturn for $q \rightarrow 0$; i.e., S_T is higher than expected. This may be due to the aggregates, which may differ from sample to sample as mentioned before. Moreover, we compare here S_T, corresponding to h-PSSNa in the solvent needed for the ZAC method (29% H_2O and 71% D_2O), and S_1, corresponding to a mixture of h-PSSNa and d-PSSNa in the same solvent. It is thus possible that the aggregates are partially masked in S_1 because of the ZAC conditions (which should kill interchain correlations), and not masked at all in S_T, leading to the observed increase in the low q region of the curve.

The curve S_T/S_1 concerning lanthanum in the redissolution area however looks different for $q \rightarrow 0$ as $S_T/S_1 > 1$. This redissolution results from the screening of the electrostatic interactions due to the high ionic strength I. If such a high I is obtained through addition of monovalent ions (NaCl), the chain conformation is close to that of the neutral chain.[6] The signal S_T/S_1 is lower than 1 for small q and increases toward 1 with q. The high S_T/S_1 increase if $q \rightarrow 0$ for high $[La^{3+}]$ concentration is thus not expected. This can result from different phenomena. A first explanation may be the aggregates. Contrary to the solutions considered above, this sample crosses the two phases region, and it may be difficult to redissolve the dense precipitated phase formed. This can result in a higher intensity of the aggregates in S_T than in S_1, solution in which the two kinds of polymer d and h precipitate together. Another hypothesis is that the polymer is in bad solvent near the threshold $[La^{3+}]_2$: the S_T/S_1 increase for small q thus results from attractive interactions, as observed in colloidal dispersions of spheres.[22] Indeed, if La^{3+} is increased above $[La^{3+}]_2$, the increase of intensity still exists although it is smaller, which is consistent with a better quality of the solvent far from this $[La^{3+}]_2$ threshold.

The choice between these two explanations is however difficult to assess, and it would be necessary to perform specific experiments. This is moreover closely related to the precise nature of aggregates, a question which is not clear and still under debate concerning polyelectrolytes.[23−26] It would here for example be interesting to study the influence of filtering after the salt has been added or to prepare several samples at the same concentration to check the reproducibility.

6. Comparison of the Addition of Multivalent Ions to the Addition of Monovalent Ions

6.1. Checks of the Monovalent Case. As mentioned in the Introduction, several authors have studied PSSNa with or without added sodium ions. We have also performed some measurements with added NaBr in order to compare the influence of multivalent and monovalent ions on the same chains. We first recall our measurements with Na^+ ions, which lead to several remarks concerning the absolute value of both a and l_p.

First, our data treatment and fitting procedure gives a around 1.7 Å. This is smaller than the former value from the same group, determined from the slope $1/a$ of the asymptote,[1−3] but it is in agreement with the value found in ref 4 by a different group, determined from the length of short chains that behave like rods. Despite the fact that the methods used to determine a are different, the obtained values should be the same if the WLC holds. Another puzzling point is that this value of 1.7 Å is smaller than what is expected given the monomer size. The result $a = 1.7$ Å has been extensively discussed in ref 4, but its origin is not clear.

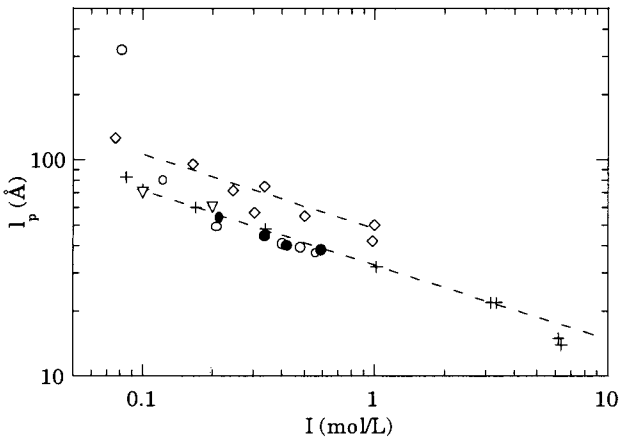

Figure 8. Plot of the persistence length l_p of PSSNa without and with added monovalent ions vs the ionic strength I calculated without condensation. The different symbols correspond to data from different studies. White circles, ref 1; black circles, ref 2; crosses, ref 3; reversed triangles, ref 4; white diamonds, this study. The dashed lines correspond to an $I^{-0.33}$ variation.

Second, the values obtained for l_p are larger in the present study than in other works. Once a is known, l_p is extracted from the value of $al_p = 1/q^2S_1$. The latter is related to the concentration of the polymer, to the contrast, and to the absolute intensity. The polymer concentration is experimentally determined. The contrast is calculated using the same value than previous works. The absolute intensity will then be a crucial value that influences both a and l_p: it depends on a numerical factor obtained from the measurement of $d\sigma/d\Omega_{water}$. If we consider our ensemble of data, it is noticeable that $d\sigma/d\Omega$ as well as the values of a and l_p determined from several solutions and different scattering experiments are rather reproducible: for example, for repeated measurements at $c_p = 0.3$ M and no added salt, we always find $a = 1.6-1.7$ Å and $l_p = 54-58$ Å. (From such experiments, we estimate that the error on a is 0.05 and that the error on l_p is around 5%.) This corresponds to a value of 92.3 ± 0.5 for al_p. The values obtained by others for a are different ($a = 2$ and $l_p = 46$ Å in ref 3) but lead to $al_p = 92$, a value very close to our average given above. This agrees with the fact that our a is smaller but our l_p is larger.

Anyhow, the variations of the persistence lengths with ionic strength are roughly the same for the different works: the electrostatic persistence length $l_e = l_p - 12$ Å varies like $I^{-0.5}$ and the total one l_p varies like $I^{-0.33}$. The variation of the experimental persistence length l_p obtained in several studies including the present one vs the ionic strength I has been reported in Figure 8.

6.2. Comparisons for the Radius of Gyration. Let us first look at the consistency of the different R_g determinations. The R_g values given in Tables 1−3 are obtained from the small q extrapolation of the data using eq 2. In the framework of the WLC model, the radius of gyration should also obey eq 6, implying l_p and a. Equation 6 leads to $R_{g,calc}$ values smaller than the experimental determination $R_{g,meas}$, even if some polydispersity is introduced, following the formula given in ref 1, and whatever the valence of the added ions. For example, the $R_{g,meas} = 180$ Å for PSSNa with $c_p = 0.3$ mol/L and no added salt, while $R_{g,calc} = 146$ Å using the values $a = 1.7$ Å and $l_p = 55$ Å determined from the fit of the whole curve. Notice that several works[1,4] directly

Table 3. Comparison of the Chain Characteristics of PSSNa for Identical Ionic Strengths Obtained with Several Ionic Compositions[a]

	salt (mol/L)	l_p (Å)	R_g (Å)	d_i (Å)	I'' (mol/L)
$c_p = 0.3$	Na = 0.11	55	180	14.9	0.16
$I = 0.25$	Ca = 0.037	52	158	16.1	0.12
	La = 0.021	49	154	16.5	0.09
$c_p = 0.3$	Na = 0.34	42	162	11.9	0.39
$I = 0.5$	Ca = 0.11	36	148	13.8	0.27
	La = 0.053	nw	121	15.2	0.19
$c_p = 0.165$	Na = 0.42	50	141	11.8	0.45
$I = 0.5$	Ca = 0.14	39	136	14.1	0.15
$c_p = 0.076$	Na = 0.085	72	204	18.8	0.1
$I = 0.12$	Ca = 0.028	62	166	21.7	0.07

[a] c_p is the polymer concentration (mol/L), the ionic strength I equals $c_p + 2c_s$ (mol/L), "nw" means that the chain is not wormlike, d_i is the distance between ions, and I'' is the ionic strength calculated with condensed counterions.

replace $R_{g,calc}$ in eq 5 by $R_{g,meas}$ to determine l_p. Doing so here for the above example with $R_{g,meas} = 180$ Å would lead either to $l_p = 90$ Å if keeping $a = 1.7$ Å or to $a = 2.5$ Å if keeping $l_p = 55$ Å. The determined conformation would thus be quite different.

We can attempt the same comparison between $R_{g,meas}$ and $R_{g,calc}$ in former studies. It is not possible to conclude for refs 2 and 5 because the values of R_g are not given. In ref 3, $R_{g,calc}$ is smaller than $R_{g,meas}$, exactly as in the present study. This result seems thus to be a general trend, which is not related to the valence of the ions. It probably results from the presence of aggregates as explained in section 2.5. Let us remark that works[1,4] that can extract the conformation of short chain only from $R_{g,meas}$ do not mention the aggregates. This does not imply that these results are wrong: aggregates may not be visible either because short chains aggregate less or because one can use larger scattering vectors for the determination of R_g.

Finally, let us note that both estimates of R_g anyhow lead to the same conclusions. The experimental values of the radius of gyration for a given ionic strength I show that R_g decreases; i.e., the chain is more compact, while increasing the cation valence (see Table 3). The $R_{g,calc}$ values obtained from l_p and a, although smaller than $R_{g,meas}$, also decrease under the same changes.

6.3. Multivalent Cations Added to PSSNa: Ionic Strength *I*. The l_p values both for monovalent and multivalent cations are plotted in Figure 9a as a function of I (without condensation). First, for Na^+ ions as well as low concentrations of Ca^{2+} and La^{3+}, the chain remains wormlike and l_p roughly varies as $I^{-1/3}$. Second, for high Ca^{2+} concentrations, the chain is no longer wormlike; nevertheless, we observe that the l_p values still follow $l_p \sim I^{-1/3}$. However, the range available for the l_p variation is too limited to observe a clear departure from the $I^{-1/3}$ law. Third, for La^{3+} ions, the chain is no longer wormlike as soon as we depart from the very low concentration range; we see that the values of l_p pertain to a different "branch" and are much lower than along the main "branch". This latter behavior is in agreement with the macroscopic precipitation observed. Finally, for high La^{3+} concentrations in the soluble range, l_p is close to the measurements with other cations since it returns to the value of the neutral chain whatever the type of added salt.

It has nevertheless to be noticed that the l_p values tend to be slightly smaller for multivalent cations than for monovalent ones (see Figure 9a and Table 3), an observation which is consistent with the decrease of R_g observed in parallel.

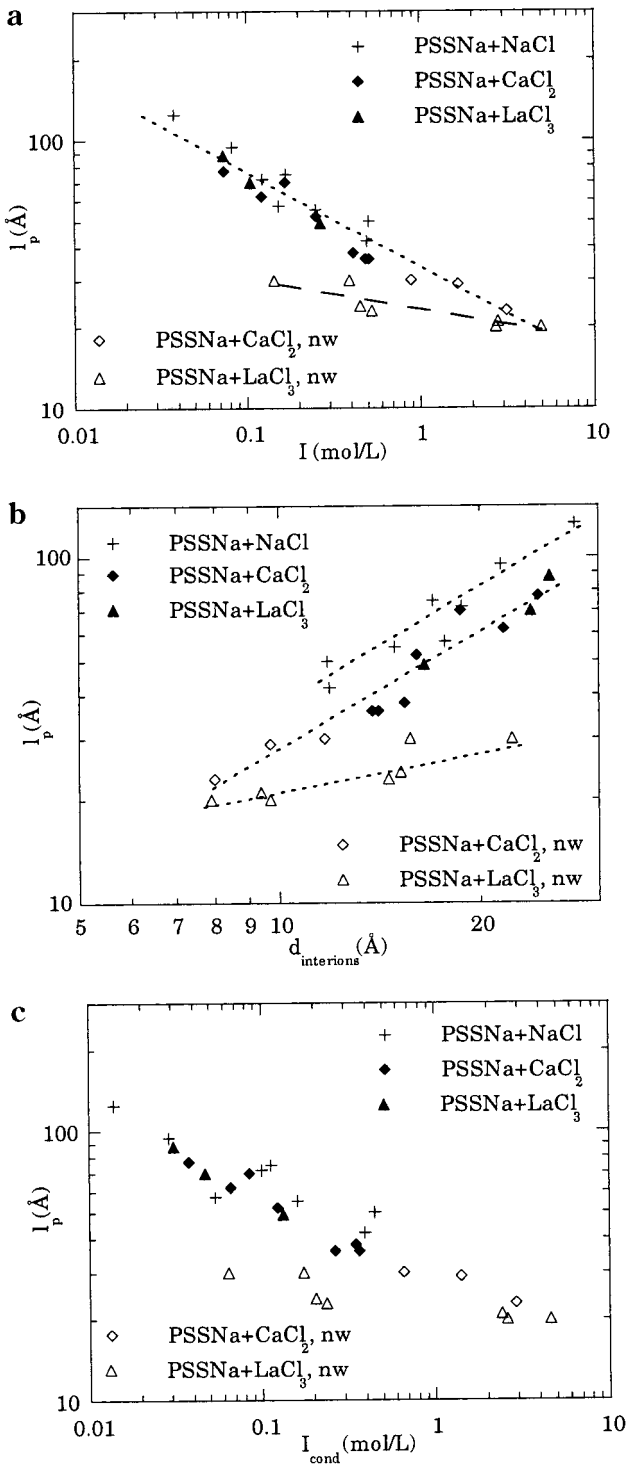

Figure 9. (a) Persistence length l_p vs ionic strength I. (b) l_p vs the distance $d_{interions}$ between ions. (c) l_p vs I_{cond} calculated with condensation. Black symbols correspond to wormlike chains whereas white symbols correspond to the nonwormlike (nw) chains. The lines are guides for the eye.

The ionic strength I may thus not be the only parameter controlling l_p: while increasing the valence at a given I, the chain becomes more flexible and more compact. Moreover, its conformation progressively deviates from the wormlike chain model.

6.4. Multivalent Cations: Other Variables. As it seems that the ionic strength is not the only parameter

controlling l_p, let us now look for other variables. It was suggested in ref 3 that $l_p \sim I^{-0.33}$ may correspond to a variation like the distance d_i between ions. This distance, which is given by d_i (Å) $= 10^9(1/N_a/c_{ions}$ (mol/L)), where c_{ions} is the total concentration of ions in the solution, is reported in Table 3. The graph l_p vs d_i is plotted in Figure 9b. Concerning the case when the WLC applies, it shows that the l_p values for multivalent ions are shifted compared to the l_p values for Na^+. Indeed, for a given ionic strength, c_{ions} decreases with the valence of the ions, leading to larger distances d_i between ions and thus to a shift of the data. The distance d_i thus does not seem to control l_p.

Another possibility is to plot l_p vs I_{cond}, ionic strength with condensation. Calculating I_{cond} only affects the samples with no added salt or low salt concentrations because the change due to condensation is negligible in the other cases. The use of I_{cond} thus only shifts some of the points. Figure 9c shows that the correlation is not improved.

The differences between the three ions could also result from their size. Nevertheless, their bare sizes are close (see Appendix), and evaluating the size of the hydrated ions is a very delicate task because it depends on many parameters, among them the condensation of the ion.

It should be noted also that the ionic strength is a mean-field concept, which forgets about local effects which could occur for a valency larger than one. However, the ionic strength I used at the beginning appears to be still the best parameter to correlate the persistence lengths.

6.5. Nonwormlike Chains. For high enough salt concentrations of Ca^{2+} or La^{3+}, there is always a deviation from the wormlike chain model. It is probably associated with a conformation change of the polymer in the presence of multivalent ions. Before any clear deviation from the WLC, a already decreases a little. For high salt concentrations, if we try to fit curves at high q, even if the fit is not correct over the whole q range, we need to use even smaller a (1.4 or 1.3 Å). This would correspond to a higher apparent weight per unit length and suggests that the chain may become thicker. We can also consider that the model of wormlike chain with no thickness used here may therefore no longer be convenient.

A first level of accounting for the thickness of the chain is to introduce a factor $\exp(-q^2R_c^2/2)$ multiplying the form factor S_1, R_c being the radial dimension of the chain (a kind of 2D transversal radius of gyration). This term has little influence for small q but greatly modifies the curves for large scattering vectors.[27] In particular, the scattered intensity now varies like $q^{-1}\exp(-q^2R_c^2/2)$ instead of q^{-1} at large q. Hence, it leads us to change our criteria for the background subtracted in the data treatment; now the value to subtract depends on the size R_c chosen. This treatment thus generates two additional fitting parameters. We nevertheless tried it for the curves that disagreed with the simple wormlike model, but it does not improve the fit. Consequently, we believe that the conformation of the chain is different from a thick wormlike one.

7. Conformation of the PSSCa Chain: Multivalent Counterions

As the results for PSSNa with calcium or lanthanum ions added seem to be related to the behavior of the multivalent ions toward the polymer chain, we studied a system with no monovalent ions. The polymer charges are directly compensated by multivalent counterions, and multivalent ions can also be added. Experiments are possible for PSSCa only, because the solutions in water are stable at least at room temperature, at variance with the case of PSSLa,[9] the latter being insoluble.

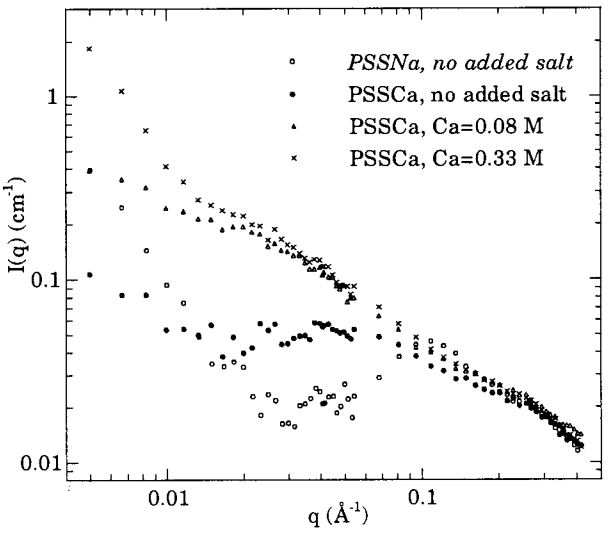

Figure 10. Scattered intensity of PSSCa solutions without and with added Ca^{2+} ions; the calcium concentrations are given in the legend. PSSNa without salt is plotted for comparison. $c_p = 0.3$ mol/L for all curves.

7.1. Total Scattering. Let us first consider the *total signal* S_T for PSSCa without and with added $CaCl_2$ plotted in Figure 10. The curve for PSSNa at the same polymer concentration is plotted on the same graph for comparison. The curves are very different: the existence of a peak is very clear for PSSNa but not for PSSCa. It nevertheless seems that there is a smooth peak for much lower q than for PSSNa. This makes the peak closer to the signal of the aggregates, which are also clearly present in these samples and which probably partially mask the peak.

A first reason for the displacement of the q_{max} value is related to the Debye length κ^{-1}. For the same polymer concentration $c_p = 0.3$ mol/L, and without added salt, $I = 0.15$ mol/L for PSSNa and $I = 0.3$ mol/L for PSSCa. The higher ionic strength for PSSCa corresponds to a smaller κ^{-1} that would induce a larger q_{max}, contrary to what is observed. If condensation is taken into account, I_{cond} is the same for both solutions, i.e., κ^{-1} also, and this disagrees with the data, too. A second explanation would imply that this peak corresponds to a mean distance between chain segments, if the solution is considered as a chain lattice. This implies a different conformation for PSSCa chains: as the polymer concentration is the same for PSSCa and PSSNa, a smaller q_{max} may mean that the distance between chains is larger; i.e., the chains are thicker so that their total length is shorter.

7.2. Intrachain Scattering. Let us now focus on the *form factor* S_1 in Figure 11 for the same PSSCa and $CaCl_2$ concentrations as Figure 10, with PSSNa for comparison. From a qualitative point of view, the influence of the addition of salt is the same than for the previous experiments with PSSNa: $q^2S_1(q)$ increases at a given q. However, even the curves at $c_p = 0.3$ mol/L with no added salt are very different for PSSNa and

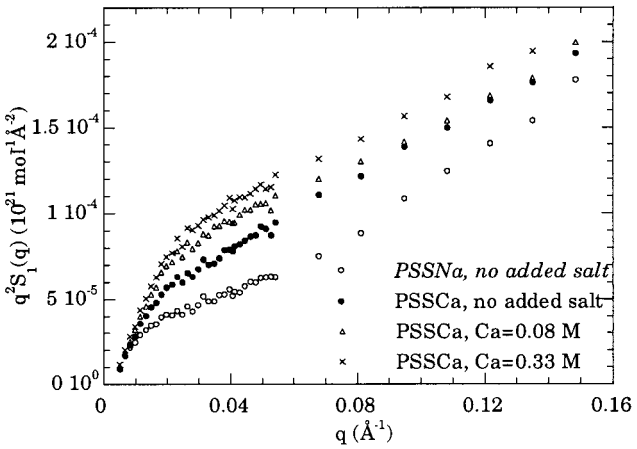

Figure 11. Kratky representation for PSSCa without and with added Ca^{2+} ions; the calcium concentrations are given in the legend. PSSNa without salt is plotted for comparison. c_p = 0.3 mol/L for all curves.

PSSCa. For PSSCa, the chain appears to be locally much more flexible or at least more coiled. This should not be the case if I_{cond} is the right parameter, since the I_{cond} values are identical for both polymers at the same c_p without salt. Conversely, the value of I itself is higher for PSSCa, which is indeed more flexible. This could suggest that the condensation has not to be taken into account to calculate the ionic strength, i.e., that the ions behave as if they were free in the solution, in agreement with previous results.[3] Of course, we forget here possible effects of bridging for divalent ions, which can also decrease the apparent l_p.

From a quantitative point of view, we cannot determine l_p because the curves for PSSCa do not follow the wormlike chain model, *even with no added salt*. The deviations from the model are the same as what was observed and previously described for multivalent ions added to PSSNa (see Figure 1d). The comparison of $q^2S_1(q)$ for different solutions with the same I nevertheless leads to the conclusion that the ionic strength is here not the right parameter: the results show that the chain is all the more flexible and compact as the proportion of Ca^{2+} ions increases. This conformation change is thus related to the presence of multivalent ions.

8. Conformation of the PSS Chain with Multivalent Ions: Discussion

8.1. Description of the Conformation. Our experimental study allows us to follow the chain conformation in all the monophasic areas for different cations valence. We propose in Figure 12 a schematic description of the chain in the different cases. In this figure, the undulation at small scale is related to the value of a while the one at larger scales is related to l_p.

We distinguish two regimes (as visible in the variation of l_p (I), Figure 9a):

(i) For small I, the behavior is quite similar for cations of any valence: the chain apparently remains wormlike (Figure 12). For diluted enough multivalent ions, the bridging interactions could occur between monomers distant from each other along the chain. Such loops are not appearing in addition to the "natural" loops of a wormlike chain.

(ii) For larger I, the chain keeps a WLC conformation with Na^+ ions. Conversely, for multivalent ions, when increasing I, not only l_p decreases but also the weight per unit length $1/a$ increases, thus leading to a "thicker" chain. At the same time, the chain progressively deviates from the wormlike chain model. If trying to fit the curves with this model, we conclude that the chain is more expanded than a WLC given its rigidity (l_p) (see Figure 12). One striking feature is the similarity of the behaviors for Ca^{2+} and La^{3+} cations. In the one-phase region, although these similar behaviors are observed for lower La^{3+} concentrations than for Ca^{2+}, conformations found are very similar; meanwhile, Ca^{2+} induces no separation contrary to La^{3+}.

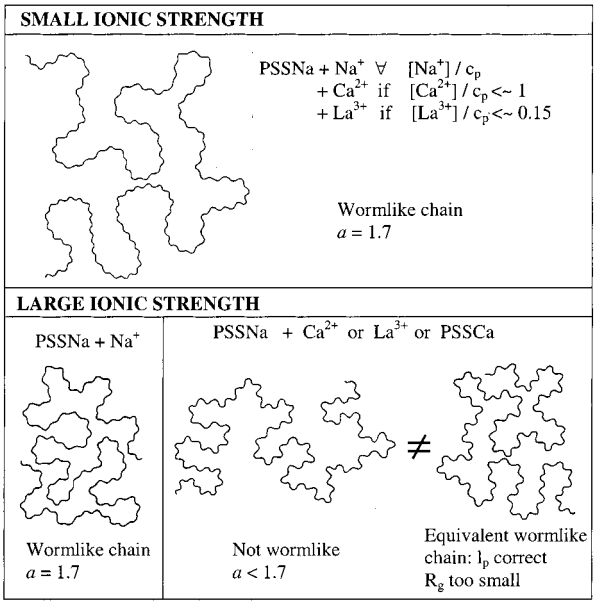

Figure 12. Schematic description of the conformation of the chain in all the monophasic areas for the different cations valence (see text for details).

8.2. Comparison with Theoretical Descriptions. The addition of cations to poly(styrenesulfonate), which bears anionic groups, has two consequences. First, the cations interact with the anionic groups: this attraction increases with the valence of the cation, z_{ci}. Second, the added salt increases the ionic strength and thus contributes to electrostatic screening, which, for a given ionic concentration c_{ions}, also increases with z_{ci}. Consequently, the electrostatic interaction that increases with z_{ci} is also more screened if z_{ci} increases. Both phenomena vary differently with c_{ions}, and the resulting conformation of the chain depends on the balance between them.

A first well-known account of this attraction/screening balance is simply the Manning condensation:[13,14] the cations condensation increases with z_{ci} (at constant rodlike conformation); hence, the effective ionic strength, I_{cond}, is lower than I, and the screening is reduced. This disagrees with experimental data:

(i) For low I, the conformation seems to be ruled mostly by the global ionic strength: $l_p \sim I^{-1/3}$. One does not get a more consistent variation of the data by looking at the variation of l_p with I_{cond}. Changing from mono- to di- or trivalent, i.e., increasing z_{ci} at given I, should decrease I_{cond} and *increase* the persistence length l_p: this is *not* seen here.

(ii) For larger I, l_p also clearly varies in opposite direction compared to the predictions. Another mechanism could be evoked: for large z_{ci}, like 3, condensation could make the polymer charge weak enough to meet the conditions of existence of an electrostatic blob;[28] i.e., the polymer is locally Gaussian and stretched only above ξ_{el}. This could result in an apparent decrease of l_p but

cannot be detected in our data, which show that the conformation remains close to the wormlike chain.

Following a second theoretical attempt, the ion−chain attraction results in chain−chain ion bridging: the condensation of the cations on a fraction of the monomers creates on the chain some positive charges among negative charges, thus some attraction between different monomers which is short range, so that it is called bridging.[9,10] This short-range character allows to define an effective interaction parameter χ_{el} and hence an apparent excluded volume $\nu_{el} \sim (1 - 2\chi_{el})$. Then a mean-field derivation of the phase diagram is in good agreement with observation: experiments on PSS show that such an electrostatically driven phase separation occurs if the cations are at least trivalent. In short, as for a classical polymer solution around the Θ temperature, the theory considers a balance between the entropy of mixing of the chains and the enthalpy of mixing described by χ_{el}. The conformation of one single chain in the one-phase region, not explicitly considered in these studies,[9,10] may remain unaffected close to phase separation. Individual collapse cannot occur before phase separation: it would occur only in conditions similar to neutral polymer solutions, i.e., in dilute solution far below Θ temperature.

Our experimental data suggest that ion bridging acts only at the local scale on the conformation but does not produce loops or collapse. Also, we see qualitatively similar conformation for single chains for divalent and trivalent cations. The evolution from Ca^{2+} to La^{3+} is only quantitative: the contraction is stronger but qualitatively similar to Ca^{2+}. This could be surprising since theories predict a very different effect in divalent and trivalent case: locally, ion bridging would dominate screening only for $z_{ci} > 2$ (i.e., $\nu_{el} > 0$, resulting in attraction only in this case). If theories were wrong, ν_{el} could be negative for Ca^{2+} and phase separation could occur for higher molecular weight or lower temperature. Otherwise, the possibility remains that there is a regime where ν_{el} decreases for the two types of cations but never becomes negative for Ca^{2+}.

A third description can be found in numerical simulation of the conformation. In their simulations Stevens and Kremer[7] consider only monovalent cations, but they have also varied the range of the electrostatic attraction, by varying the Bjerrum length l_B, which is rather similar to increase the valence of the cations. The simulations performed show a very interesting point: the chain contracts if l_B increases. Condensation modifies the conformation and this all the more as the cation valence increases. Stevens et al. simulations are in agreement with some of our observations: the decrease of a corresponds to a contraction at the local scale. At larger scale, l_p and R_g decrease also; the fact that R_g is larger than its WLC value suggests that the contraction is mostly local. But this requires a more detailed explanation.

In summary, the progressive local contraction of the chain can be attributed to condensation or to local "ion bridging", which would in both cases increase progressively with the added cation valence.

Finally, another point of view is to imagine that the decrease of a could also be due to an inhomogeneous thickening of the chain, reminiscent of the pearl necklace model of Dobrynin et al.[29] that has been developed for polyelectrolytes in bad solvent. A possible agreement with Dobrynin's model has been observed for partially charged $PSSNa_x$, the form factor signaling a partly globular shape.[6] This seems different here, where data do not show any clear size of pearl. To end this discussion, let us stress that we do not know of any model that could fit the experimental curves at present.

9. Conclusions

SANS experiments have been here performed on fully charged PSS chains in the presence of cations of valences between 1 and 3: PSSNa with Na^+, Ca^{2+}, or La^{3+} ions added and PSSCa without and with Ca^{2+} ions added. As observed in previous works,[8,9] no macroscopic changes occur with Na^+ and Ca^{2+}, but the solution separates in two phases with La^{3+}, in good agreement with a theory of ion bridging. The use of the ZAC method allows to follow the chain conformation, thus the microscopic behavior, that has not been seen before in the macroscopic studies that focused on the phase behavior.

Our results may be separated in two regimes depending on the value of the ionic strength I.

For low ionic strength (Figure 12) in PSSNa solutions, the conformation does not change; i.e., the chain remains wormlike. As explained in the Introduction, the addition of multivalent cations allows to vary differently I, I_{cond} (ionic strength taking condensation into account), and d_i (distance between ions). The results show that the persistence length l_p roughly varies as $I^{-1/3}$, like for monovalent ions. In other words, condensation is not visible. These results lead to the conclusion that I is the best parameter (although a slight shift in the l_p values has to be accounted for).

For higher ionic strength (Figure 12) added to PSSNa solutions and for PSSCa solutions, progressive changes occur. With multivalent ions, the chain progressively deviates from the wormlike chain model: (i) the weight per unit length $1/a$ decreases, meaning that the chain is "thicker"; (ii) given its rigidity, the chain is more expanded (R_g is larger) than expected in the framework of the wormlike chain model. Contrary to the case of low I values, the ionic strength I is no longer the only parameter controlling the conformation. This conformation change is opposite to the predictions of Manning's condensation. It may result either from bridging between monomers or from an influence of the counterions condensation on the chain. It is however difficult to differentiate between these two hypotheses. An important point is the qualitative similarity of the conformation for Ca^{2+} and La^{3+} ions added although the macroscopic behaviors are different (phase separation for La^{3+} and not for Ca^{2+}). This results from a different balance of attraction and screening for the two cations: in both cases the excluded volume decreases, but for Ca^{2+}, it never becomes negative. Nevertheless, trends are the same for both cations compared to monovalent cations, thus leading to the same kind of conformations.

The improvement of the knowledge of the conformation will necessitate more experiments, among them the study of dilute PSSCa:

(i) From the experimental point of view, the results clearly show that the aggregates, undissolved polymer or living aggregates, are a nuisance for the conformation determinations because of their contribution to the scattered intensity for small scattering vectors. In the second case, their origin and their characteristics are however not well understood yet, and they would necessitate a special and precise study. Another im-

Table 4. Characteristics of the Different Counterions[a]

counterions	Na^+	Ca^{2+}	La^{3+}
R_{ion} (Å)	0.95	1	1.06
b_s (10^{12} cm)	1.31		
b_i (10^{12} cm)	0.363	0.49	0.827
$k^2_{Ci,naked}$ (10^{24} cm^2)	0.042	0.094	0.37
partial molal vol (cm^3/mol)	−6.6	−28.6	−55.3
$k^2_{Ci,hydrated}$ (10^{24} cm^2)	0.48	5.4	23

[a] R_{ion} is the radius of the ion, b_s is the coherent scattering length of the used solvent (29% H_2O/71%D_2O), b_i is the coherent scattering length of the ions, $k^2_{Ci,naked}$ is the contrast calculated for the bare ion, and $k^2_{Ci,hydrated}$ is the contrast calculated for a hydrated ion (see Appendix for details).

provement may be the use of shorter chains that should lead to fewer aggregates.

(ii) From the theoretical point of view, we lack a theoretical model for the description of the chains.

Acknowledgment. We thank P. Lixxon (Service de Chimie Moléculaire, CEA-Saclay) for the COT measurements of titration of the polymer concentration in solutions, J. P. Cotton (LLB), C. Treiner, and M. Rawiso (Institut Ch. Sadron, Strasbourg) for fruitful discussions and finally B. Demé (Inst. Laue Langevin, Grenoble) for his time, his help, and his kindness on D22 and D11 at ILL.

Appendix: Contrast of the Counterions

The intensity scattered by a polyelectrolyte solution can be written

$$I(q)/\rho = k_m{}^2 S_{mm}(q) + 2k_m k_c S_{mc}(q) + k_c{}^2 S_{cc}(q)$$

where ρ is the monomer concentration, and the indices m and c respectively correspond to monomeric unit and counterion. $S_{ij}(q)$ is the $i-j$ structure function. The contrast k_i of the species i is calculated using $k_i = b_i - b_s V_i/V_s$, where b_i is the scattering length of the elementary unit of species i, V_i is its volume, b_s is the average scattering length of the solvent molecules, and V_s is their volume. The monomer−monomer structure function S_{mm} decomposes into $S_1 + \rho S_2$, where S_1 is the intrachain signal and S_2 is the interchain signal. For a mixture of 50% PSH chains (contrast $k_m{}^H$) and 50% PSD chains (contrast $k_m{}^D$), the intensity can be written

$$I(q)/\rho = 0.5(k_m{}^{D^2} + k_m{}^{H^2})S_1 + 0.25\rho(k_m{}^D + k_m{}^H)^2 S_2 + (k_m{}^D + k_m{}^H)k_c S_{mc} + k_c{}^2 S_{cc}$$

In the conditions of the zero average contrast (ZAC) method (see section 2.4), $k_m{}^H = -k_m{}^D$, and $I(q)/\rho = k_m{}^{H^2} S_1 + k_c{}^2 S_{cc}$. The scattered intensity is proportional to S_1 only if the contrast k_c of the counterion is negligible compared to the contrast $k_m{}^H$ of the polymer[4] or if $k_m{}^{H^2} S_1 \gg k_c{}^2 S_{cc}$. Therefore, the contrast of the counterion k_c must be evaluated.

Estimation of the Contrast of the Counterions. A first way is to calculate a contrast $k_{Ci,\ naked}$ by considering the isolated ion, using its diffusion length b_i and its radius R_i extracted from literature: b_i, R_i, and $k^2_{Ci,naked}$ values are given in Table 4. A second way is to calculate a contrast $k_{Ci,hydrated}$ by considering the ion surrounded by its solvatation shell[30] of n water molecules. It must be emphasized that, whatever n, $k_{Ci,naked} = k_{Ci,hydrated}$ when no electrostriction occurs, id est the volume of bound water molecules is the same as the normal water molecules:

$$k_{Ci,hydrated} = (b_i + nb_s) - b_s(V_i + nV_s)/V_s = b_i - b_s V_i/V_s$$

Conversely, if electrostriction occurs, the structure of water, and thus its volume, is modified around the ion. The partial molal volumes that quantify electrostriction are given in Table 4: it is negative for the three ions and highly increases with the valence. Under a very simple assumption, the change of volume can be attributed equally to the n water molecules,[30] giving a new molar volume V'_s per water molecules in the hydration shell. If the change of volume for a water molecule is noted ΔV, this leads to the formula

$$k_{Ci,hydrated} = k_{Ci,naked} + nb_s(1 - V'_s/V_s) = k_{Ci,naked} + nb_s(\Delta V/V_s)$$

A first difficulty is to determine the number n of water molecules. As ΔV varies as $1/n$, $k_{Ci,hydrated}$ is independent of n and the precise value of n does not matter. A second difficulty is that the partial molal volume is given for low salt concentrations, while our experiments are in a much more concentrated regime. Also, the meaning of the calculated change of volume becomes doubtful when it is large, in particular for multivalent ions: for example, putting $n = 6$ water molecules in the hydration shell for La^{3+} ions, the calculation gives $V'_s = 9$ cm^3/mol for the molar volume of water molecules instead of 18 cm^3/mol. Nevertheless, we give in Table 4 the $k^2_{Ci,hydrated}$ values resulting from this very simple calculation.

Estimation of the Contribution of the Cations to the Intensity. Concerning the counterions, their contrast has to be compared to $k_m{}^H$ for the polymer. In our experiments (50% PSH, 50% PSD, and H_2O 29%/D_2O 71%, i.e., $b_s = 1.31 \times 10^{-12}$ cm), the contrast $k_m{}^{H^2}$ equals 13.3×10^{-24} cm^2 for the poly(styrenesulfonate) in the conditions of the zero-averaged contrast method. If we consider $k^2_{Ci,naked}$, the contribution of counterions is negligible. If we consider $k^2_{Ci,hydrated}$, only Na^+ ions still have a negligible contribution. Nevertheless, it is very difficult to rely on these $k^2_{Ci,hydrated}$ values for the reasons evoked above; another important reason is that the hydration may change if the ions are condensed or not on the polymer chain.

Let us first consider free ions in the solution: their contribution can be written $k^2/VP(q)S(q)$, where V is the volume of the ions, $P(q)$ is the form factor of the ion, i.e., $P(q) \sim 1$ in the explored q range, and $S(q)$ is the structure factor. $S(q)$ tends toward 1 at large q and should be smaller than 1 for small q if there is no aggregation. Therefore, in a rough evaluation, the contribution of ions should be of the order of k^2/V. For *small q*, this must be compared to the contribution Nk^2/V of the polymer: thus, the contribution of the ions is negligible. Conversely, for *large q*, the contribution of the ions may no longer be negligible. Nevertheless, this large q contribution is taken into account when subtracting the blank spectrum (no polymer) (see section 2.5) that was always measured with a salt concentration equivalent to the one of added salt in the solution.

Besides, the blank measurements show that the level of the background with salt is very close to the level of

the background without salt and always slightly smaller. The calculation of the variation of this level with La^{3+} ions depends on the hypothesis on hydration. If La^{3+} is assumed to be hydrated, the background level is expected to increase with salt, whereas if it is naked, the level is nearly the same. The measured background levels thus favor the hypothesis of naked counterions as scatterers.

To stress important points, and to conclude, we can say that the contrast of counterions is negligible in absence of electrostriction, whereas it could be important for La^{3+} in the presence of electrostriction. The counterions correlation term S_{cc} would then become visible and could interfere with the changes observed at large q in the presence of Ca^{2+} or La^{3+}. We do not think that this would be the only reason for these changes, since for example PSSCa shows larger effects than PSSNa + Ca and also since changes are observed at the level of the global size (for small q). Also, the data we have for electrostriction are for dilute salt solutions, and it should decrease noticeably at large concentration and most probably in the presence of polymer. Finally, we have no sign of this in absence of polymer, for the blanks, where the hydration should be the most important (whereas it could decrease when ions are linked or close to the polyion).

References and Notes

(1) Nierlich, M.; Boué, F.; Lapp, A. *J. Phys. (Paris)* **1985**, *46*, 649.
(2) Nierlich, M.; Boué, F.; Lapp, A.; Oberthür, R. *Colloid Polym. Sci.* **1985**, *263*, 955.
(3) Spiteri, M. N.; Boué, F.; Lapp, A.; Cotton, J. P. *P. R. L.* **1996**, *77*, 5218.
(4) Kassapidou, K.; Jesse, W.; Kuil, M. E.; Lapp, A.; Egelhaaf, S.; van der Maarel, J. R. C. *Macromolecules* **1997**, *30*, 2671.
(5) Nishida, K.; Urakawa, H.; Kaji, K.; Gabrys, B.; Higgins, J. S. *Polymer* **1997**, *38*, 6083.
(6) Spiteri, M. N. Ph.D. Thesis, Université d'Orsay, Paris XI, 1997; Chapter 2.
(7) Stevens, M. J.; Kremer, K. *J. Chem. Phys.* **1995**, *103*, 1669.
(8) Axelos, M. A. V.; Mestdagh, M. M.; François, J. *Macromolecules* **1994**, *27*, 6594.
(9) Olvera de la Cruz, M.; Belloni, L.; Delsanti, M.; Dalbiez, J. P.; Spalla, O.; Drifford, M. *J. Chem. Phys.* **1995**, *103*, 5781.
(10) Raspaud, E.; Olvera de la Cruz, M.; Sikorav, J. L.; Livolant, F. *Biophys. J.* **1998**, *74*, 381.
(11) Sabbagh, I. Ph.D. Thesis, Université d'Orsay, Paris XI, 1997.
(12) Vink, H. *Makromol. Chem.* **1980**, *182*, 279.
(13) Oosawa, F. In *Polyelectrolytes*; Dekker: New York, 1971.
(14) Manning, G. S. *Ber. Bunsen-Ges. Phys. Chem.* **1996**, *100*, 909.
(15) Brulet, A.; Boué, F.; Cotton, J. P. *J. Phys. (Paris)* **1996**, *6*, 885.
(16) Boué, F.; Cotton, J. P.; Lapp, A.; Jannink, G. *J. Chem. Phys.* **1994**, *101*, 2562.
(17) Sharp, P.; Bloomfield, V. A. *Biopolymers* **1968**, *6*, 1201.
(18) des Cloizeaux, J. *Macromolecules* **1973**, *6*, 403.
(19) Joanny, J. F.; Barrat, J. L. *Adv. Chem. Phys.* **1996**, *XCIV*, 1.
(20) Williams, C.; Nierlich, M.; Cotton, J. P.; Jannink, G.; Boué, F.; Daoud, M.; Farnoux, B.; Picot, C.; de Gennes, P. G.; Rinaudo, M.; Moan, M.; Wolff, C. *J. Polym. Sci., Polym. Lett. Ed.* **1979**, *17*, 381.
(21) Essafi, W.; Lafuma, F.; Williams, C. E. *Eur. Phys. J. B* **1999**, *9*, 261.
(22) Woutersen, A. T. J. M.; May, R. P.; de Kruif, C. G. *J. Colloid Interface Sci.* **1992**, *151*, 410.
(23) Ghosh, S.; Peitzsch, R. M.; Reed, W. F. *Biopolymers* **1992**, *32*, 1105.
(24) Sedlak, M. *Macromolecules* **1993**, *26*, 1158.
(25) Smits, R. G.; Kuil, M. E.; Mandel, M. *Macromolecules* **1994**, *27*, 5599.
(26) Ermi, B. D.; Amis, E. J. *Macromolecules* **1998**, *21*, 7378.
(27) Rawiso, M.; Duplessix, R.; Picot, C. *Macromolecules* **1987**, *20*, 630.
(28) Pfeuty, P. *J. Phys. (Paris)* **1978**, *39*, CII-149.
(29) Dobrynin, A.; Rubinstein, M.; Obukhov, S. P. *Macromolecules* **1996**, *29*, 2974.
(30) Heinrich, M. Ph.D. Thesis, Université Louis Pasteur, Strasbourg, 1998.

MA000956U